\



Tri-hexagonal charge order in kagome metal CsV_3Sb_5 revealed by ^{121}Sb nuclear quadrupole resonance

Chao Mu(牟超), Qiangwei Yin(殷蔷薇), Zhijun Tu(涂志俊), Chunsheng Gong(龚春生), Ping Zheng(郑萍), Hechang Lei(雷和畅), Zheng Li(李政), and Jianlin Luo(雒建林)

Citation: Chin. Phys. B, 2022, 31 (**1**): 017105. DOI: 10.1088/1674-1056/ac422c
Journal homepage: http://cpb.iphy.ac.cn; http://iopscience.iop.org/cpb

What follows is a list of articles you may be interested in

Pressure tuning of the anomalous Hall effect in the kagome superconductor CsV_3Sb_5

Fang-Hang Yu(喻芳航), Xi-Kai Wen(温茜凯), Zhi-Gang Gui(桂智刚), Tao Wu(吴涛), Zhenyu Wang(王震宇), Zi-Ji Xiang(项子雾), Jianjun Ying(应剑俊), and Xianhui Chen(陈仙辉)

Chin. Phys. B, 2022, 31 (**1**): 017405. DOI: 10.1088/1674-1056/ac3990

High-magnetic-field induced charge order in high-T_c cuprate superconductors

L X Zheng(郑立玄), J Li(李建), T Wu(吴涛)

Chin. Phys. B, 2019, 28 (**11**): 117402. DOI: 10.1088/1674-1056/ab4575

Nuclear magnetic resonance measurement station in SECUF using hybrid superconducting magnets

Zheng Li(李政), Guo-qing Zheng(郑国庆)

Chin. Phys. B, 2018, 27 (**7**): 077404. DOI: 10.1088/1674-1056/27/7/077404

Direct observation of melted Mott state evidenced from Raman scattering in 1T-TaS_2 single crystal

Qing Hu(胡庆), Cong Yin(尹聪), Leilei Zhang(张雷雷), Li Lei(雷力), Zhengshang Wang(王正上), Zhiyu Chen(陈志禹), Jun Tang(唐军), Ran Ang(昂然)

Chin. Phys. B, 2018, 27 (**1**): 017104. DOI: 10.1088/1674-1056/27/1/017104

High sensitivity refractive index gas sensing enhanced by surface plasmon resonance with nano-cavity antenna array

Zhao Hua-Jun

Chin. Phys. B, 2012, 21 (**8**): 087104. DOI: 10.1088/1674-1056/21/8/087104

SPECIAL TOPIC — Superconductivity in vanadium-based kagome materials

Tri-hexagonal charge order in kagome metal CsV_3Sb_5 revealed by ^{121}Sb nuclear quadrupole resonance

Chao Mu(牟超)[1,2], Qiangwei Yin(殷蔷薇)[3], Zhijun Tu(涂志俊)[3], Chunsheng Gong(龚春生)[3], Ping Zheng(郑萍)[1], Hechang Lei(雷和畅)[3,†], Zheng Li(李政)[1,2,‡], and Jianlin Luo(雒建林)[1,2,4]

[1] *Beijing National Laboratory for Condensed Matter Physics and Institute of Physics, Chinese Academy of Sciences, Beijing* 100190, *China*
[2] *School of Physical Sciences, University of Chinese Academy of Sciences, Beijing* 100190, *China*
[3] *Department of Physics and Beijing Key Laboratory of Opto-electronic Functional Materials & Micro-nano Devices, Renmin University of China, Beijing* 100872, *China*
[4] *Songshan Lake Materials Laboratory, Dongguan* 523808, *China*

(Received 25 October 2021; revised manuscript received 9 December 2021; accepted manuscript online 11 December 2021)

We report ^{121}Sb nuclear quadrupole resonance (NQR) measurements on kagome superconductor CsV_3Sb_5 with T_c = 2.5 K. ^{121}Sb NQR spectra split after a charge density wave (CDW) transition at 94 K, which demonstrates a commensurate CDW state. The coexistence of the high temperature phase and the CDW phase between 91 K and 94 K manifests that it is a first order phase transition. The CDW order exhibits tri-hexagonal deformation with a lateral shift between the adjacent kagome layers, which is consistent with $2 \times 2 \times 2$ superlattice modulation. The superconducting state coexists with CDW order and shows a conventional s-wave behavior in the bulk state.

Keywords: charge-density-wave systems, nuclear magnetic resonance

PACS: 74.25.nj, 71.45.Lr, 76.60.Gv, 76.60.−k **DOI:** 10.1088/1674-1056/ac422c

The newly discovered superconductor AV_3Sb_5 (A = K, Rb, Cs) possesses a quasi-two-dimensional kagome structure, which provides a platform to investigate the interplay of topology, electron correlation effects and superconductivity.[1–5] They undergo a charge density wave (CDW) transition at T_{CDW} = 78 K, 103 K, 94 K and a superconducting transition at T_c = 0.93 K, 0.92 K, 2.5 K for A = K, Rb, Cs, respectively. The superconducting state is found to be spin singlet with s-wave pairing symmetry in the bulk state.[6–8] STM studies observed possible Majorana modes[9] and pair density wave[10] in the surface state. A residual density of states was experimentally observed in the superconducting state,[11] which may be due to the competition between the superconductivity and the CDW.[11–16]

The CDW order breaks time-reversal symmetry[17–19] and leads to the anomalous Hall effect in the absence of magnetic local moments.[20–23] Inelastic x-ray scattering and Raman scattering exclude strong electron–phonon coupling driven CDW,[24] while optical spectroscopy supports that the CDW is driven by nesting of Fermi surfaces.[25] STM experiment find the CDW peak intensities at $3Q$ which breaks the six-fold rotational symmetry.[26] An additional unidirectional 1×4 superlattice is observed on the surface,[10,27–29] but is absent in the bulk state.[30] The "star of David" (SoD) and "tri-hexagonal" (TrH) structure configurations were proposed to be the likely candidates for the CDW structures,[31,32] as illustrated in Figs. 2(b) and 2(c). SoD or TrH with a lateral shift between the adjacent Kagome layer results in a $2 \times 2 \times 2$ structure modulation.[33] Density functional theory calculations showed that the TrH deformation is preferred.[31,32,34] However, there is still lack experimental evidence whether SoD or TrH deformation is the ground state configuration in the CDW state.

In this work, we report nuclear quadrupole resonance (NQR) investigations on CsV_3Sb_5. The splitting of ^{121}Sb spectra demonstrates that a commensurate CDW order forms at 94 K with a first-order transition. Our results indicate that the charge order has a tri-hexagonal deformation which is 2×2 period modulation. The shift between the adjacent kagome layers induces a modulation in the c-direction and the CDW is a three-dimensional modulation with $2 \times 2 \times 2$ period. Spin–lattice relaxation rate measured at the peak of the CDW state shows a coherence peak just below T_c, indicating that the superconducting state coexists with the CDW order and shows a conventional s-wave behavior.

Single crystals of CsV_3Sb_5 were synthesized using the self-flux method.[6] Superconductivity with T_c = 2.5 K was confirmed by dc magnetization measured using a superconducting quantum interference device (SQUID). The NQR measurements were performed using a phase coherent spectrometer. The spectra were obtained by frequency step and sum method which sums the Fourier transformed spectra at a series of frequencies.[35] The spin–lattice relaxation time T_1 was measured using a single saturation pulse. Crystal structures were visualized in VESTA.[36]

[†]Corresponding author. E-mail: hlei@ruc.edu.cn
[‡]Corresponding author. E-mail: lizheng@iphy.ac.cn

© 2022 Chinese Physical Society and IOP Publishing Ltd

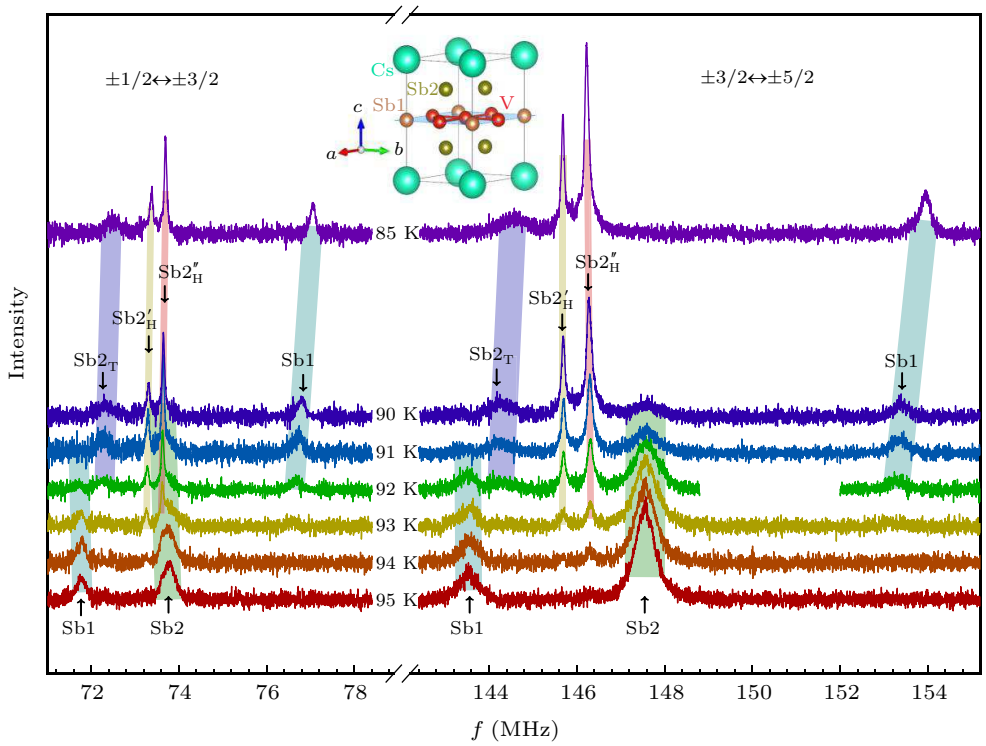


Fig. 1. The ^{121}Sb-NQR spectra around T_{CDW}. The peaks in the low frequency range are from $\pm 1/2 \leftrightarrow \pm 3/2$ transition and the peaks in the high frequency range are from $\pm 3/2 \leftrightarrow \pm 5/2$ transition. There are 2 sites of Sb marked by Sb1 and Sb2 above T_{CDW}. Both peaks of Sb2 split due to non-equivalent sites emerging below T_{CDW}. The notations of Sb1, $Sb2'_H$, $Sb2''_H$ and $Sb2_T$ are consistent with those in Fig. 2(c). The spectra of all temperatures are presented in the supplemental material.

Figure 1 shows the NQR spectra of ^{121}Sb in zero field. There are two different crystallographic sites of Sb in CsV_3Sb_5 with the atomic ratio of Sb1 : Sb2 = 1 : 4. Sb1 is located in the V-kagome plane, and Sb2 forms a graphite-like network between V-kagome layers, as shown in the inset of Fig. 1 and Fig. 2(a). It is easy to distinguish Sb2 peaks from Sb1 peaks by the spectral intensity. The nuclear spin Hamiltonian of the interaction between quadrupole moment Q and the electric field gradient (EFG) is described as

$$\mathcal{H}_Q = \frac{h\nu_Q}{6}\left[(3I_z^2 - I^2) + \frac{\eta}{2}(I_+^2 + I_-^2)\right], \quad (1)$$

where ν_Q is the quadrupole resonance frequency along the principal axis (c-axis), $\nu_Q \equiv \frac{3e^2qQ}{2I(2I-1)}$, with $eq = V_{zz}$. η is an asymmetry parameter of the EFG, $\eta = (V_{xx} - V_{yy})/V_{zz}$, where V_{xx}, V_{yy}, V_{zz} are the EFGs along the x, y, z directions, respectively. ^{121}Sb with $I = 5/2$ has two NQR peaks for each site, $|\pm\frac{1}{2}\rangle \leftrightarrow |\pm\frac{3}{2}\rangle$ transition at low frequency and $|\pm\frac{3}{2}\rangle \leftrightarrow |\pm\frac{5}{2}\rangle$ transition at high frequency.

Four NQR transition peaks can be clearly identified above 95 K. Below $T_{CDW} = 94$ K, the intensity of the original peaks decreases gradually and four sets of new peaks emerge, indicating that the CDW transition is commensurate and four unequal sites of Sb atoms appear in the CDW state. The coexistence of two phases between 91 K and 94 K demonstrates that the CDW transition is of first-order due to a simultaneous superlattice transition.[2] It is consistent with NMR studies on ^{51}V which also show coexistent behavior.[6,37,38] The peaks below T_{CDW} are complex and cannot be distinguished by the intensity alone.

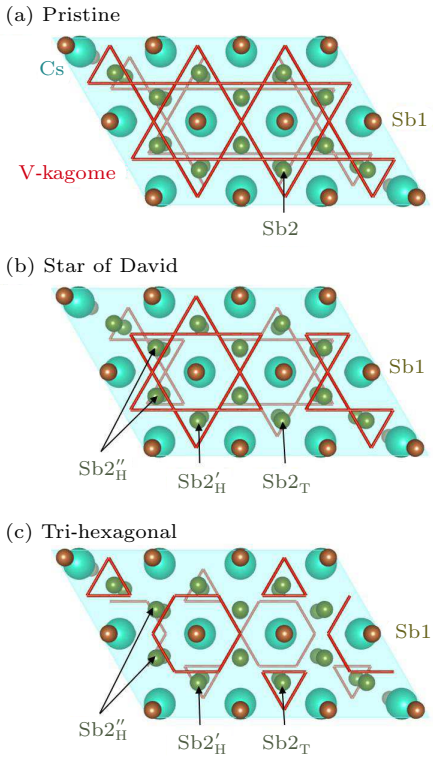


Fig. 2. Perspective view of crystal structures of CsV_3Sb_5 in (a) the pristine phase, (b) the star of David phase and (c) the tri-hexagonal phase. There is a shift between adjacent layers in the star of David configuration and the tri-hexagonal configuration.

Two structure configurations named as "star of David" and "tri-hexagonal" have been proposed in the CDW state.[31,32,34] We can assign the $Sb2_H$ and $Sb2_T$ sites by their symmetry. In SoD configuration, as shown in Fig. 2(b), $Sb2_H$ is inside the star and $Sb2_T$ is outside the star. In TrH configuration, as shown in Fig. 2(c), $Sb2_T$ is located at the center of the trigonal V-network and $Sb2_H$ is outside. A lateral shift between the adjacent kagome layers forms modulation on the c-axis,[33,34] which results in a nematic state with only C_2 rotation symmetry and makes $Sb2'_H$ site different from $Sb2''_H$ site.[39] The subscript "H" denotes the sites around the hexagon and the subscript "T" denotes the sites at the triangle center. The four new peaks in Fig. 1 correspond to these four sites, Sb1, $Sb2'_H$, $Sb2''_H$ and $Sb2_T$. The spin-lattice relaxation time T_1 is employed to track the evolution of the peaks. $1/T_1T$ of the peak around 77 MHz evolutes from Sb1, as shown in Fig. 3. $1/T_1T$ of the peaks around 74 MHz marked by $Sb2'_H$ and $Sb2''_H$ are the same and evolute from Sb2, see Fig. 2 in Ref. [6]. The peak around 72 MHz has a weak intensity and T_1 measurement has large uncertainty just below T_{CDW}. Fortunately, there is only $Sb2_T$ site left, so the peak around 72 MHz is attributed to it. In addition, the asymmetry parameter η can also be used to distinguish them.

All peak positions are summarized in Figs. 4(a)–4(d). Combining the frequencies of $|\pm\frac{1}{2}\rangle \leftrightarrow |\pm\frac{3}{2}\rangle$ transition and $|\pm\frac{3}{2}\rangle \leftrightarrow |\pm\frac{5}{2}\rangle$ transition, ν_Q and η are calculated, as shown in Figs. 4(b), 4(c), 4(e), and 4(f). The η at all sites is zero above T_{CDW}, reflecting the isotropy of EFG in the xy-plane. Below T_{CDW}, η of Sb2 changes to finite values, indicating that the in-plane symmetry is broken and unequal sites of Sb2 are generated. The slightly decreasing ν_Q implies that the main change is not the EFG strength, but the EFG direction at Sb2 sites. On the other hand, Sb1 in kagome plane has high symmetry, so the EFG at Sb1 site changes frequency obviously without asymmetry. When the electric field modulation period is twice the lattice constant, the highly symmetrical sites are not affected by the modulation,[40] so the Sb1 peak does not split like the Sb2 peak.

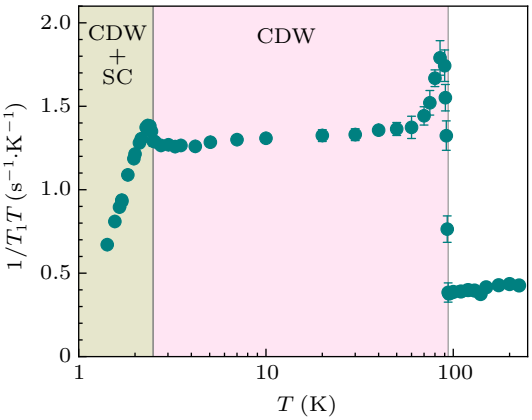


Fig. 3. Temperature dependence of $^{121}(1/T_1T)$ of Sb1 site. $1/T_1T$ jumps at T_{CDW}. A Hebel–Slichter coherence peak appears just below T_c.

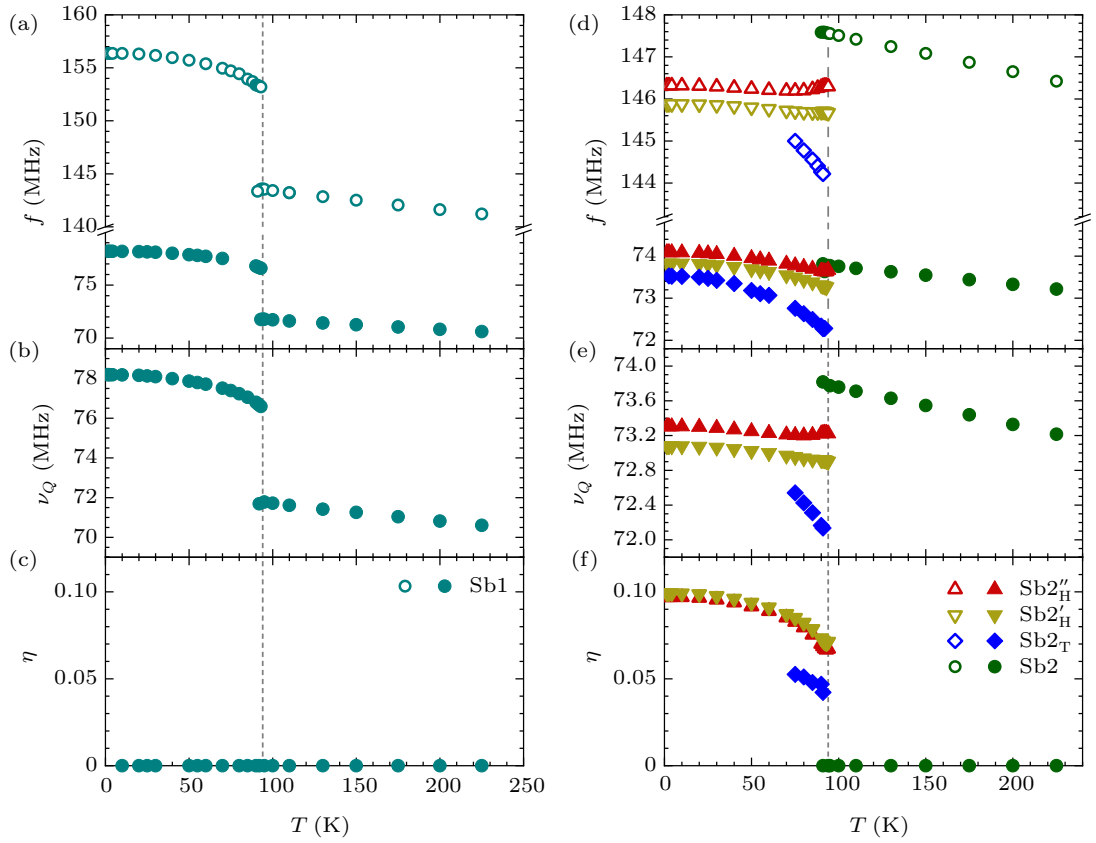


Fig. 4. Temperature dependence of (a), (d) peak positions, (b), (e) ν_Q and (f), (g) η of Sb1 site and Sb2 site, respectively. The vertical dashed lines indicate the transition temperature of CDW.

Next, we will distinguish between the two configurations of TrH and SoD. The CDW has a three-dimensional modulation and the modulation in c-axis will make Sb2 plane have different pattern from the kagome plane. Therefore, the different between TrH and SoD in the kagome plane should be detected by Sb1 rather than Sb2. In TrH deformation, V atoms are closer to Sb1 site, so ν_Q of Sb1 moves a lot toward high frequency, as shown in Fig. 4(b). In SoD deformation, on the other hand, V atoms move away from Sb1 site, so ν_Q of Sb1 should not increase, which is inconsistent with the NQR spectra. The $Sb2_H$ peaks split to $Sb2'_H$ and $Sb2''_H$ peaks due to a lateral shift between adjacent layers in the tri-hexagonal configuration. The intensity ratio of the two peaks is 1 : 2, which is consistent with the atoms ratio. NQR frequency is determined by EFG, so the NQR spectra indicates that the electronic modulation pattern is formed simultaneously with the structural distortion. Our results favor TrH deformation over SoD deformation and are consistent with $2a \times 2a \times 2c$ pattern. If $4a$ pattern exists, it should only exist on the surface.[30,32]

The ν_Q and η jump at T_{CDW} and then change gradually in the CDW state. They remain constant when entering the superconducting state, indicating the coexistence of superconductivity and the CDW order. $^{121}(1/T_1T)$ measured at the peak in the CDW order state shows superconducting transition, as shown in Fig. 3, confirming the coexistence. $^{121}(1/T_1T)$ shows a clear Hebel–Slichter coherence peak just below T_c and then rapidly decreases at low temperatures, as shown in Fig. 3, indicating that CsV_3Sb_5 is a conventional s-wave superconductor. It is consistent with our previous result measured at Sb2 site.[6]

In conclusion, we have performed ^{121}Sb NQR studies on CsV_3Sb_5. The variation of the NQR spectra indicates a first-order commensurate CDW transition at 94 K. We identified four Sb sites in the CDW state which give restriction on the CDW order. The charge order can be understood in terms of tri-hexagonal deformation with lateral shift between the adjacent kagome layers, which has a $2 \times 2 \times 2$ period. In the superconducitng state, $^{121}(1/T_1T)$ of Sb1 site in kagome planes shows conventional s-wave behavior, just as $^{121}(1/T_1T)$ of Sb2 site between kagome planes. The superconducting phase coexists with CDW order in the bulk state.

Acknowledgments

Project supported by the National Key Research and Development Program of China (Grant Nos. 2017YFA0302901, 2018YFA0305702, 2018YFE0202600, and 2016YFA0300504), the National Natural Science Foundation of China (Grant Nos. 12134018, 11921004, 11822412, and 11774423), the Beijing Natural Science Foundation, China (Grant No. Z200005), and the Strategic Priority Research Program and Key Research Program of Frontier Sciences of the Chinese Academy of Sciences (Grant No. XDB33010100).

References

[1] Ortiz B R, Gomes L C, Morey J R, Winiarski M, Bordelon M, Mangum J S, Oswald I W H, Rodriguez-Rivera J A, Neilson J R, Wilson S D, Ertekin E, McQueen T M and Toberer E S 2019 *Phys. Rev. Materials* **3** 094407
[2] Ortiz B R, Teicher S M L, Hu Y, Zuo J L, Sarte P M, Schueller E C, Abeykoon A M M, Krogstad M J, Rosenkranz S, Osborn R, Seshadri R, Balents L, He J and Wilson S D 2020 *Phys. Rev. Lett.* **125** 247002
[3] Ortiz B R, Sarte P M, Kenney E M, Graf M J, Teicher S M L, Seshadri R and Wilson S D 2021 *Phys. Rev. Materials* **5** 034801
[4] Yin Q W, Tu Z J, Gong C S, Fu Y, Yan S H and Lei H C 2021 *Chin. Phys. Lett.* **38** 037403
[5] Jiang K, Wu T, Yin J X, Wang Z, Hasan M Z, Wilson S D, Chen X and Hu J 2021 Preprint arXiv: 2109.10809
[6] Mu C, Yin Q, Tu Z, Gong C, Lei H, Li Z and Luo J 2021 *Chin. Phys. Lett.* **38** 077402
[7] Xu H S, Yan Y J, Yin R, Xia W, Fang S, Chen Z, Li Y, Yang W, Guo Y and Feng D L 2021 *Phys. Rev. Lett.* **127** 187004
[8] Duan W, Nie Z, Luo S, Yu F, Ortiz B R, Yin L, Su H, Du F, Wang A, Chen Y, Lu X, Ying J, Wilson S D, Chen X, Song Y and Yuan H 2021 *Science China Physics, Mechanics & Astronomy* **64** 107462
[9] Liang Z, Hou X, Zhang F, Ma W, Wu P, Zhang Z, Yu F, Ying J J, Jiang K, Shan L, Wang Z and Chen X H 2021 *Phys. Rev. X* **11** 031026
[10] Chen H, Yang H, Hu B, Zhao Z, Yuan J, Xing Y, Qian G, Huang Z, Li G, Ye Y, Ma S, Ni S, Zhang H, Yin Q, Gong C, Tu Z, Lei H, Tan H, Zhou S, Shen C, Dong X, Yan B, Wang Z and Gao H J 2021 *Nature* **599** 222
[11] Zhao C C, Wang L S, Xia W, Yin Q W, Ni J M, Huang Y Y, Tu C P, Tao Z C, Tu Z J, Gong C S, Lei H C, Guo Y F, Yang X F and Li S Y 2021 Preprint arXiv: 2102.08356
[12] Chen K Y, Wang N N, Yin Q W, Gu Y H, Jiang K, Tu Z J, Gong C S, Uwatoko Y, Sun J P, Lei H C, Hu J P and Cheng J G 2021 *Phys. Rev. Lett.* **126** 247001
[13] Yu F H, Ma D H, Zhuo W Z, Liu S Q, Wen X K, Lei B, Ying J J and Chen X H 2021 *Nat. Commun.* **12** 3645
[14] Du F, Luo S, Ortiz B R, Chen Y, Duan W, Zhang D, Lu X, Wilson S D, Song Y and Yuan H 2021 *Phys. Rev. B* **103** L220504
[15] Zhang Z, Chen Z, Zhou Y, Yuan Y, Wang S, Wang J, Yang H, An C, Zhang L, Zhu X, Zhou Y, Chen X, Zhou J and Yang Z 2021 *Phys. Rev. B* **103** 224513
[16] Chen X, Zhan X, Wang X, Deng J, Liu X B, Chen X, Guo J G and Chen X 2021 *Chin. Phys. Lett.* **38** 057402
[17] Jiang Y X, Yin J X, Denner M M, Shumiya N, Ortiz B R, Xu G, Guguchia Z, He J, Hossain M S, Liu X, Ruff J, Kautzsch L, Zhang S S, Chang G, Belopolski I, Zhang Q, Cochran T A, Multer D, Litskevich M, Cheng Z J, Yang X P, Wang Z, Thomale R, Neupert T, Wilson S D and Hasan M Z 2021 *Nat. Mater.* **20** 1353
[18] Shumiya N, Hossain M S, Yin J X, Jiang Y X, Ortiz B R, Liu H, Shi Y, Yin Q, Lei H, Zhang S S, Chang G, Zhang Q, Cochran T A, Multer D, Litskevich M, Cheng Z J, Yang X P, Guguchia Z, Wilson S D and Hasan M Z 2021 *Phys. Rev. B* **104** 035131
[19] III C M, Das D, Yin J X, Liu H, Gupta R, Wang C N, Jiang Y X, Medarde M, Wu X, Lei H C, Chang J J, Dai P, Si Q, Miao H, Thomale R, Neupert T, Shi Y, Khasanov R, Hasan M Z, Luetkens H and Guguchia Z 2021 Preprint arXiv: 2106.13443
[20] Yang S Y, Wang Y, Ortiz B R, Liu D, Gayles J, Derunova E, Gonzalez-Hernandez R, Šmejkal L, Chen Y, Parkin S S P, Wilson S D, Toberer E S, McQueen T and Ali M N 2020 *Science Advances* **6** eabb6003
[21] Kenney E M, Ortiz B R, Wang C, Wilson S D and Graf M J 2021 *J. Phys.: Condens. Matter* **33** 235801
[22] Yu F H, Wu T, Wang Z Y, Lei B, Zhuo W Z, Ying J J and Chen X H 2021 *Phys. Rev. B* **104** L041103
[23] Feng X, Jiang K, Wang Z and Hu J 2021 *Science Bulletin* **66** 1384
[24] Li H, Zhang T T, Yilmaz T, Pai Y Y, Marvinney C E, Said A, Yin Q W, Gong C S, Tu Z J, Vescovo E, Nelson C S, Moore R G, Murakami S, Lei H C, Lee H N, Lawrie B J and Miao H 2021 *Phys. Rev. X* **11** 031050
[25] Zhou X, Li Y, Fan X, Hao J, Dai Y, Wang Z, Yao Y and Wen H H 2021 *Phys. Rev. B* **104** L041101

[26] Jiang Y X, Yin J X, Denner M M, Shumiya N, Ortiz B R, Xu G, Guguchia Z, He J, Hossain M S, Liu X, Ruff J, Kautzsch L, Zhang S S, Chang G, Belopolski I, Zhang Q, Cochran T A, Multer D, Litskevich M, Cheng Z J, Yang X P, Wang Z, Thomale R, Neupert T, Wilson S D and Hasan M Z 2021 *Nat. Mater.* **20** 1353

[27] Zhao H, Li H, Ortiz B R, Teicher S M L, Park T, Ye M, Wang Z, Balents L, Wilson S D and Zeljkovic I 2021 *Nature* **599** 216

[28] Liang Z, Hou X, Zhang F, Ma W, Wu P, Zhang Z, Yu F, Ying J J, Jiang K, Shan L, Wang Z and Chen X H 2021 *Phys. Rev. X* **11** 031026

[29] Wang Z, Jiang Y X, Yin J X, Li Y, Wang G Y, Huang H L, Shao S, Liu J, Zhu P, Shumiya N, Hossain M S, Liu H, Shi Y, Duan J, Li X, Chang G, Dai P, Ye Z, Xu G, Wang Y, Zheng H, Jia J, Hasan M Z and Yao Y 2021 *Phys. Rev. B* **104** 075148

[30] Li H, Jiang Y X, Yin J X, Yoon S, Lupini A R, Pai Y, Nelson C, Said A, Yang Y M, Yin Q W, Gong C S, Tu Z J, Lei H C, Yan B, Wang Z, Hasan M Z, Lee H N and Miao H 2021 Preprint arXiv: 2109.03418

[31] Ortiz B R, Teicher S M L, Kautzsch L, Sarte P M, Ruff J P C, Seshadri R and Wilson S D 2021 *Phys. Rev. X* **4** 041030

[32] Tan H, Liu Y, Wang Z and Yan B 2021 *Phys. Rev. Lett.* **127** 046401

[33] Miao H, Li H X, Meier W R, Huon A, Lee H N, Said A, Lei H C, Ortiz B R, Wilson S D, Yin J X, Hasan M Z, Wang Z, Tan H and Yan B 2021 *Phys. Rev. B* **104** 195132

[34] Ratcliff N, Hallett L, Ortiz B R, Wilson S D and Harter J W 2021 *Phys. Rev. Mater.* **5** L111801

[35] Clark W G, Hanson M E, Lefloch F and Ségransan P 1995 *Rev. Sci. Instruments* **66** 2453

[36] Momma K and Izumi F 2011 *Journal of Applied Crystallography* **44** 1272

[37] Song D W, Zheng L X, Yu F H, Li J, Nie L P, Shan M, Zhao D, Li S J, Kang B L, Wu Z M, Zhou Y B, Sun K L, Liu K, Luo X G, Wang Z Y, Ying J J, Wan X G, Wu T and Chen X H 2021 Preprint arXiv: 2104.09173

[38] Luo J, Zhao Z, Zhou Y Z, Yang J, Fang A F, Yang H T, Gao H J, Zhou R and Zheng G Q 2021 Preprint arXiv: 2108.10263

[39] Ni S, Ma S, Zhang Y, Yuan J, Yang H, Lu Z, Wang N, Sun J, Zhao Z, Li D, Liu S, Zhang H, Chen H, Jin K, Cheng J, Yu L, Zhou F, Dong X, Hu J, Gao H J and Zhao Z 2021 *Chin. Phys. Lett.* **38** 057403

[40] Li Z, Jiao W H, Cao G H and Zheng G Q 2016 *Phys. Rev. B* **94** 174511